

Interactive learning environment for diagnostic radiography with real-time X-ray simulation and patient positioning

Aaron Sujar^{a,b}, Graham Kelly^{c,b}, Luis Pastor^a, Marcos García^{a,*}, Franck P.Vidal^b

^a*Grupo de Modelado y Realidad Virtual, Universidad Rey Juan Carlos, Spain*

^b*Bangor University, United Kingdom*

^c*Shrewsbury and Telford Hospital NHS Trust, United Kingdom*

Abstract

We present an interactive learning environment for diagnostic radiography. Our aim is to provide a validated software that can be used to teach radiography using real-time interactive X-ray simulation. Patient positioning can be performed by rotating any joint of the virtual patient. The tool can be used within a lecture to illustrate cases of interest, show specific errors, the effect of the X-ray machine parameters, etc., that would have been difficult (if not impossible) to encounter during the training due to the harmful nature of ionising radiations. We adapted a fast and accurate character animation technique so that the user can import any kind of anatomic models, move the joints of the virtual patient into the required position, and deform the skin surface and the internal soft tissues accordingly. gVirtualXRay, an open source library to simulate X-rays, is used to generate the corresponding radiographs in realtime. Parameters of the X-ray machine, e.g. beam collimation, beam spectrum, etc. can also be changed by the user and the effect of the changes are visualised without delay. A face and content validation study has been conducted. 18 participants were recruited to evaluate our software using a questionnaire. The results show that our tool is realistic in many ways (72% of the participants agreed that the simulations are visually realistic), useful (67%) and suitable (78%) for teaching X-ray radiography. It is a vital aspect of undergraduate training that mistakes are learnt from to ensure they are not replicated within the real clinical setting. However, trainees are not allowed any mistake in patients due to the use of ionising radiations. Our interactive learning environment for diagnostic radiography enables educators to bridge the disconnects between theory and practice by using a virtual X-ray room within the classroom without using real patients and avoiding any kind of radiation risk.

Keywords: Real-time simulation, interactive simulation, character animation, interactive learning environment, X-rays, diagnostic radiography

1. Introduction

Projectional radiography (also called projection radiography, and X-ray radiography) is a very common medical imaging tool that supports clinicians in the diagnostic of certain diseases, infections, injuries (e.g. bone fractures), and to locate foreign objects. It can be used in almost every part of the patient's body although each specific body location requires a given patient position and X-ray machine set up, in particular collimation of the X-ray source, voltage of the X-ray

tube, time of exposure, distance source to patient, and distance source to detector or film.

Undergraduate radiographer training within the UK is a mix of academic theory and clinical practice. Trainee radiographers learn theoretical information such as anatomy and radiation physics. Theoretical information is learnt within the classroom setting however, many institutions utilise creative simulations in order for the trainee to experience the clinical environment within a non-clinical setting such as the university. Depending on the university facilities trainees also x-ray phantom anatomy in order to further their understanding of radiation physics principles without the risk of biological damage to living tissue. Trainees can then see the effect of imaging principles such as exposure factors in real-time, a practice that could not be performed on living

*Corresponding author.

Email addresses: aaron.sujar@gmail.com (Aaron Sujar), graham.kelly@nhs.net (Graham Kelly), luis.pastor@urjc.es (Luis Pastor), marcos.garcia@urjc.es (Marcos García), f.vidal@bangor.ac.uk (Franck P.Vidal)

tissue.

This approach leads to a disconnect between the theory seen in the classroom setting, and the practice seen in the X-ray room. Teaching cases are utilised within the academic setting again to demonstrate clinical cases. They are compilations of patient histories including their medical images, recorded discussions, notes and annotations. Trainees can then study well-documented cases through large image datasets. University hospitals and medical schools often build their own repositories. However, there are now more and more online public resources where radiographers can access to a vast of sets of images from any part of the human anatomy [1]. Nevertheless students cannot experiment with such static data.

Nowadays, digital technologies are more ubiquitous than ever and smartphones start to play a big role in learning. Some institutions have created mobile phone apps in which trainees can look up images and fill in questionnaires, e.g. UBC Radiology [2]. This type of resources are playing an increasing role in the curriculum of trainees in radiology and diagnostic radiography. Nevertheless, all these images show the final results and do not describe the whole procedure. Patient positioning is a key step and it cannot be easily learned from the final images. Also, as there are static images, it is not possible to modify any acquisition parameter (e.g. tube voltage) that could interactively visualise the changes in the X-ray radiographs. According to the old adage, “we learn from our mistakes”. However, trainees are not allowed any mistake in patients due to the use of ionising radiations. For safety reasons, projections obtained with different set ups never come from the same patient, hindering any possible comparison. It is a vital aspect of undergraduate training that mistakes are learnt from to ensure they are not replicated within the real clinical setting. For trainees to further understand errors, an X-ray room is required within the academic setting. The use of an anatomical phantom is also required to X-ray in order to demonstrate these errors. This cannot be easily conducted within a typical classroom setting and therefore constitutes a separate teaching session. This could lead to a disconnect between theory and practice.

Virtual reality (VR) medical simulation is playing an increasing role in the physicians’ curriculum, such as surgeons and other specialists [3, 4]. They are applied to a wide variety of medical procedures [5, 6]. Such applications are used for safe and effective training purposes. Unlike traditional methods (using cadavers, animals or mannequins), computerised simulators permit new physicians to improve and develop their non-cognitive skills in a cheap and safe environment [7]. It

is also possible to use such simulators without the close supervision of an expert.

Recent advances in computer graphics (CG) allow the development of new simulators that can be used in the apprenticeship of radiographers. In this context, it is worth to mention two computerised simulators. On one hand, [8] is a simulator for training in interventional radiology where fluoroscopy (real-time X-ray images) is used to guide a needle towards an anatomical structure. Despite of the fact that the simulator has an interactive X-ray simulation and the deformation of lung tissues, there is only one example of patient and it is only focused on the chest area. On the other hand, ProjectionVR™ is a simulator that immerses the user into a realistic 3D X-ray room to simulate the complete procedure [9]. With virtual digitised patient data, it replicates an interactive learning environment without the risk of radiation exposure to students or patients. Although it provides a variety of real cases, the greatest limitation of this tool is that users always load the same static images with the same examples and they cannot produce new X-ray images instantly. There are only pre-computed images and users are not able to re-position a particular patient or play with anatomy variations and pathologies. Another simulator, called medspace.VR, provides an immersive 3D environment [10]. Although it allows to modify the patient position, only skin and bones seem to be present in the produced X-ray images and there is a lack of variety in the anatomic models.

Patient variability is desirable so that trainees can be exposed to all kind of possibilities, e.g. from underweight to overweight patients, from babies to elderly patients. It is also beneficial for simulators to emulate specific scenarios (e.g. a detecting foreign bodies, or collapsed lung) which would have been difficult to routinely encounter as a student.

In this paper, we propose an X-ray projectional radiograph simulator that can be used as an interactive teaching and learning environment where teachers and students are able to review numerous virtual patients with the possibility to manipulate the patient positioning and the X-ray machine parameters in realtime. Our aim was to create a software that could be used in the classroom to help bridge the gap between theory and practice. Our tool was designed with the following requirements in mind:

- It could use a wide variety of existing virtual patient models.
- Users can interactively manipulate the virtual patient to the position required in any given proce-

dure.

- Users can observe the X-ray image immediately as they change the virtual patient's position, X-ray source's position or any other X-ray machine parameter.

To fulfil the requirements mentioned above, our simulator is made of three main modules: the Virtual X-ray Imaging Library (gVirtualXR), the Virtual Patient Positioning System (VPPS) and the courseware. The first one is in charge of generating the X-ray image from a triangular mesh in realtime. This module is able to simulate the most relevant X-ray configuration parameters. VPPS transforms the anatomy of a virtual patient to the desired position. It was designed to be flexible to deal with as many virtual patients as possible. With this goal in mind, our algorithm works with incomplete anatomical models (skin and bones are the minimum tissues required) and the biomechanical properties of the virtual patient tissues are not required. Finally, both modules are integrated in a courseware environment, which implements the user interface and characterises the most important steps in X-ray projectional radiography.

Section 2 details the work related to our application. It focuses on character animation and X-ray simulation. Section 3 discusses the technical choices made: Using a real-time animation of the anatomy and a real-time framework for the simulation of X-ray images. The main features of our X-ray radiograph simulator are reviewed in Section 4. Section 5 shows the final results achieved in this project. It reviews three use cases (teacher's use, student's use, and exercises). A face and content validation study is also provided (see Section 6). Section 7 provides our conclusions and discusses possible future work. Finally, Appendix 7 describes a YouTube Playlist with videos that illustrate the most important functionalities of our interactive teaching and learning environment.

2. Related Work

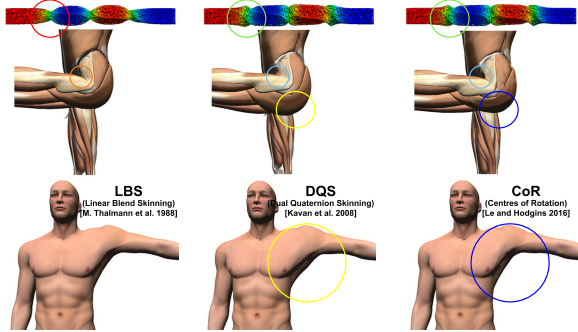
To provide the most true-to-life experience and offer a broad variety of cases, computerised medical simulators aim to be as realistic as possible. For this purpose, virtual human models are required [11]. There are commercially available anatomical virtual human models, such as ZygoteBody™ [12]. An alternative is the use of real patient data captured using medical imaging techniques such as computed tomography (CT), magnetic resonance imaging (MRI) and/or ultrasound (US). The rational is to provide more realistic models as there are

directly derived from actual patient data [13]. Although the new generation of medical simulators have recently begun to use specific patient data [14], the main problem is that those virtual patients are usually given in a specific subject position. Also, the patient's position in the medical scanner may be different from the one required by the simulator. Some particular procedures need the patient model in a different position than it was initially recorded. The consequence is that the patient data is very static and limited, and it does not represent the majority of clinical cases. Character animation from CG (i.e. techniques from the film and video game industries) can be used to move bones and update the skin surface accordingly. However, medical simulators still need a method that deals with anatomy animation including deformation of internal soft-tissues.

To animate virtual patient models as realistically as possible, we have considered bio-mechanical and musculoskeletal techniques and physically-based models from the CG literature. We can find some examples where the muscle behaviour is simulated efficiently [15]. For most of these techniques, a user must perform some steps manually and, in general, bio-mechanical models are not complete and localised only on a part of the human anatomy [16]. Others physically-based techniques try to preserve muscle's volume [17]. Muscle tissues present other problems as it is usually required to retrieve the muscle's image in relaxed and extended positions. Also, there are techniques that retrieve muscle-skeletal models from medical images [18].

All these techniques do not run at interactive rates and may require detailed information of the patient which is not readily available. Often, not all patient tissues are captured properly or the tissue's mechanical properties are not easy to extract from the medical images. Furthermore, simulators need other anatomical structures aside from simulating muscles and skeleton.

On the contrary, geometrically-based algorithms usually run in real-time and they usually produce plausible results. Skeletal animation is the most used 3D CG technique to animate articulated characters. The most widely used technique is Linear Blending Skinning (LBS) [19], but it suffers well-known artefacts such as collapsing elbows or candy wrapper effect which do not help to get realism in a simulator. Another technique commonly used is Dual Quaternion Skinning (DQS) [20], it solves LBS's problems but occasionally introduces joint-bulging artefact where meshes increase in volume. Numerous alternatives to LBS and DQS can be found in the literature [21] to address some of the deficiencies mentioned above, but at the cost of decreasing the computational performance or leading to other



(a) LBS is the classic technique but suffers from candy-wrapper artefact. (b) DQS solves candy-wrapper artefact but deformed wrapper and joint-tissues may change in volume. (c) COR is more robust to the candy from candy-wrapper fact but joint-bulging artefacts may change in bulging artefacts [23].

Figure 1: Differences between the LBS, DQS and COR skinning techniques. The red circle depicts a candy-wrapper artefact; the orange circle depicts a collapsing elbow and the yellow circles show joint-bulging artefacts. Green circles are used when candy-wrapper artefacts are solved; cyan circles when the collapsing elbow artefact is solved and blue circles when joint-bulging artefacts are solved.

artefacts. In [22], Le and Hodgins solve those artefacts without needing more computational power but a high number of centres of rotation must be initially calculated (see Figure 1).

To ease the deployment of new models by users with no or limited knowledge in CG, we have focused on methods that can provide virtual patient data automatically. Baran and Popović [24] proposed an automatic algorithm where they adapt a virtual skeleton to any 3D model. More recent work improves this method to deal with point handles, virtual bones and cages [25] (a cage defines an enclosure, using a 2D polygon or a 3D polyhedron, which is used to control the deformation of an arbitrary topology). It is also possible to use registration to transfer data from MRI to a desired anatomical model [26]. This technique is, however, not focused on animation and does not run interactively. As an alternative, Sújar *et al.* proposed a relatively similar method to deform the anatomical structures [23]. Furthermore, it is an automatic method to animate human character’s anatomy in realtime.

Another component that is required to build this interactive learning environment is the X-ray image simulator. Both accuracy and speed are requirements. Physically-based simulation frameworks exist. They are often aimed at particle physics and/or medical physics research and focus on accuracy rather than speed. These frameworks usually rely on Monte Carlo (MC) methods because they produce very realistic images [27, 28, 29].

Particles, here photons, are generated. The path of each photon through matter is tracked. At each step of the simulation, random events, such as scattering and absorption, may occur depending on probability laws that rely on the photon’s energy and the properties of the material crossed by the photon. However, MC methods are not applicable to real-time interactive applications because they have to calculate probabilistic X-ray interaction models for the transport of photons in matter and it is time consuming: To generate a relatively noise-free image, days or weeks of calculation may be needed. As a fast alternative, deterministic calculation based on ray-tracing is often used to solve the Beer-Lambert law [30, 31, 32, 33]. Freud *et al.* proposed an alternative model for deterministic simulation [34]. It relies on the traditional graphics pipeline by using a modified Z-buffer algorithm [35, 36] called L-buffer. It has been ported to the graphics processing unit (GPU) using OpenGL and its OpenGL Shading Language (GLSL) [37]. It shares the same technologies used by modern video games to provide a real-time X-ray image simulation tool. It is now available as an Open Source project, gVirtualXRay (<http://gvirtualxray.sourceforge.net/>), and can be used with various programming language such as Python, R, Ruby, GNU Octave, etc. [38]. Other GPU implementations have also been reported [39].

3. Simulator Components

We propose a tool that allows teachers and students to interact with the X-ray configuration and the patient’s positioning without any kind of radiological risk to the patient or even the radiographer. Our approach relies on two computationally intensive components: i) a real-time character animation framework (VPPS) that allows the virtual patient to change positions, with his/her internal anatomy being deformed accordingly, and ii) an X-ray simulation library (gVirtualXRay) that generates physically-based radiographic images in realtime. Besides, the courseware module integrates both components, providing a graphical interface and simulator training functions.

The VPPS precomputes a significant amount of data to achieve interactive frame rates. Fortunately, all these computations can be performed only once per model. One of the most challenging requirements we face in our research was to simplify the incorporation of new virtual patient models. Therefore, the VPPS component is split in two modules. The first one computes required pre-process data for each module and the second one

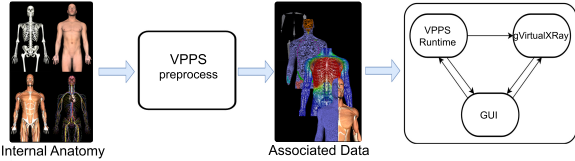


Figure 2: Simulator architecture: i) anatomical structures are pre-processed once per character, ii) then the X-Ray simulator loads the patient anatomic and the precomputed data and finally the coursework drives the training session controlling the VPPS module and gVirtualXRay. This architecture allows to run the simulation at interactive rates.

adapts the patient positioning on users demand. Figure 2 summarises the overall architecture of our software.

3.1. Virtual Patient Positioning System

To let the user select a position interactively, we adapt the internal and external anatomical models of a virtual character to any desired position. We decided to follow a purely geometrical approach based on an improved skeletal animation technique [23], instead of a fully physically-based simulation algorithm, in order to meet the following requirements:

- It has to be flexible to incorporate as many existing 3D patient models as possible.
- It has to minimize the user intervention when adding new virtual patients.
- It has to run in realtime.

Skeletal animation is commonly used in the computer graphics industry to animate articulated 3D models. This type of techniques transfers the movement of a virtual skeleton to a boundary representation (B-rep) of a virtual character. The procedure is divided into three stages: rigging, weighting and skinning. The virtual skeleton, which is a hierarchical set of virtual bones, is created in the rigging phase. The weighting phase computes the influence of each virtual bone on the model vertices. Finally, the bones' movements are transferred to the vertices through a skinning technique. The main limitation of this traditional workflow is that the rigging and weighing steps are usually performed manually by a 3D artist to provide a plausible animation. Although there exist several approaches to automatise these two steps [40, 41], they are designed to work with B-reps and they cannot be used to deform internal soft-tissues.

Our method relies on a fully automatic procedure that transfers the bone movements to all tissue models. In

contrast to classical skeletal animation techniques, our animation pipeline applies the bones movements to a Lagrangian mesh that discretises the interior of the virtual patient. We use the volumetric Lagrangian mesh to interpolate a displacement field, which is used to deform any available internal or external patient anatomy. In order to build the virtual skeleton and the volumetric Lagrangian mesh, the meshes corresponding to bones and the skin have to be correctly labelled and they are the only required tissues (i.e. internal tissues are optional). We have divided the animation workflow in five successive stages:

Rigging: We adapt a predefined virtual skeleton to the labelled bone tissue.

Volumetrisation: This stage automatically builds a volumetric Lagrangian mesh.

Weighting: Our method estimates the influence of the virtual bones on the volumetric mesh vertices, using the diffusion equation for the stationary case.

Mapping: Aiming at accelerating the real-time animation of the patient anatomy, all the virtual tissues are mapped into the volumetric mesh.

Skinning: The virtual bones movements are applied to the volumetric mesh and then transferred to the patient tissues.

The first four steps are computationally expensive and they have to be executed only once per patient. Therefore, we have grouped them in a VPPS Preprocess Module. The skinning phase is implemented to run on modern GPUs and achieves interactive frame rates, even for complex models (see Section 5).

3.2. Virtual X-ray Imaging Library

A deterministic simulation tool is required to generate images in realtime. Monte Carlo simulation is not suitable as it cannot provide real-time performance. gVirtualXRay has been selected for the X-ray generation as it is an open-source library that makes use of portable technologies, such as the C++ language, OpenGL and GLSL for the core library, and Simplified Wrapper and Interface Generator (SWIG) to generate binders to other programming languages (to-date C#, Java, Octave, Perl, Python 2 and Python 3, R, and Ruby are supported) [42]. gVirtualXRay also makes use of triangular meshes to describe the patient's anatomy. This requirement is shared with the real-time patient positioning component. This is the most common data representation in realtime 3-D graphics. Digitally reconstructed radiograph (DRR), a well-known technique to

generate radiographs from CT scans, has been discarded for this reason [43]. It is not convenient to implement a character animation model with voxel data from CT. Also, to increase performance, GPU handles on the triangular meshes are shared between gVirtualXRay and the real-time patient positioning component.

gVirtualXRay implements Freud *et al.*'s L-buffer principle [34] on the GPU. It relies on a modified rendering pipeline from 3-D computer graphics. The L-buffer aims at computing the path length of X-rays through polygon meshes, from the X-ray source to every pixel of the detector. It is then used to solve the Beer-Lambert law (also called attenuation law) from polygon meshes. It was first implemented on GPU with a monochromatic beam spectrum (all the photons have the same energy) and for parallel projections (e.g. to mimic a source far away from the scanned object as with a synchrotron) and infinitesimally small point sources [37]. Extra rendering passes (i.e. loops in the algorithm) were added to the rendering pipeline to allow the use of polychromatic beam spectra and to model the focal spot of an X-ray tube [44]. The current version of gVirtualXRay relies on the XCOM Photon Cross Sections Database from the National Institute of Standards and Technology (NIST) to compute the mass attenuation coefficient of the material of the scanned objects [45]. The material can be defined as a chemical element (e.g. hydrogen), a mixture (e.g. "Ti90Al6V4" for a titanium alloy with small amounts of aluminium, 6%, and vanadium, 4%), a compound (e.g. "H₂O" for water), or a Hounsfield unit. We chose the latter as it is commonly understood in the medical community. Hounsfield units are then converted into their respective chemical compositions and densities [46]. A quantitative validation study has been conducted to assess the accuracy of the simulated X-ray images [38]. Geant4, a state-of-the-art Monte Carlo radiation transport code by the European Organization for Nuclear Research (CERN), is used to generate some X-ray radiographs. Each image required about two weeks of computations on HPC Wales' supercomputer. Similar radiographs are simulated on the GPU with gVirtualXRay in milliseconds. Corresponding images are then compared (see Figure 3 for an example). Test images produced with gVirtualXRay are perfectly correlated with the ground-truth images produced using Geant4.

4. Courseware

The courseware is in charge of developing the training capabilities of the simulator, integrating the previously described modules and providing a graphical user

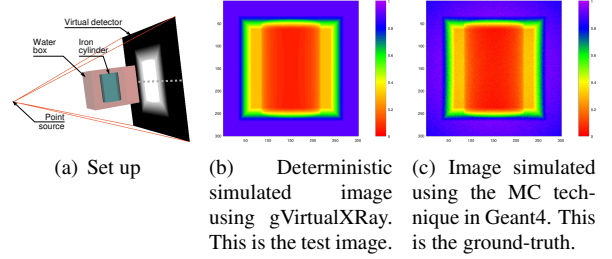


Figure 3: Example of validation test using a simple test case.



Figure 4: GUI of our projectional radiography simulator: (a) patient positioning options, (b) centring, tube voltage, source-object distance and source-cassette distance configuration (c) collimation setup, (d) tissue visibility and material properties, (e) side marker's selection and digital image manipulation.

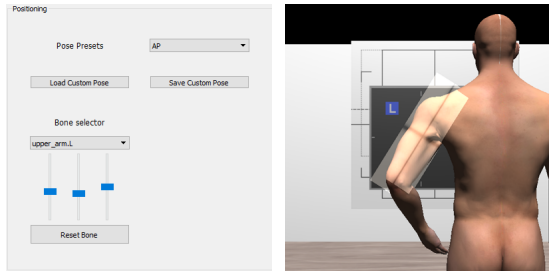
interface (GUI). Figure 4 shows how the GUI looks like and the main functionalities of the simulator. All the GUI widgets related to the position functionality are grouped in the upper left corner of the window. In the lower left corner, the X-ray machine setup can be configured. The list of patient tissues is located in the upper right corner. Finally, in the lower right corner, the corresponding X-ray image is shown and it can be modified using the mouse.

This section describes its most important features. First, we explain how the procedure is characterised and then, the lecturing and self guided-training functionalities are described.

4.1. Simulation of the X-Ray Procedure

4.1.1. Positioning the Patient

In projectional radiography, the positioning of a patient is essential in order to get the best image whilst reducing the radiation dose to the minimum requirement. As described in the radiographer curriculum [47], the users can choose if the patient is standing up or lying down. Note that the VPPS makes use of a purely geometrical algorithm and does not take into account the



(a) A user defines the left arm position via the GUI.
(b) Corresponding 3D visualisation where the virtual patient's left arm has been moved accordingly.

Figure 5: An example of virtual patient positioning.

effect of gravity. Then, users are able to define the position of a particular body part through the GUI, using a variety of methods: (i) Common positions used in radiography are preset and they can be chosen from a top-down list; (ii) They can eventually choose any body part and move it directly. The users can then modify the position of any bone by altering the rotation angles of the corresponding joints using sliders; (iii) They can estimate the position of virtual patient using motion capture with an off-the-shelf peripheral such as the Microsoft Kinect (see <https://youtu.be/1s-eTT1pCy8> for evidence). In Figure 5, the upper arm was moved to get an lateral humerus projection. Any position can be saved so that teachers can make pre-recorded positions available to students or for future use in the classroom. Depending on the lecturer demands any of the previously described techniques can be removed from the GUI. <https://youtu.be/zitw5-Xk4dY> is a link to a video that illustrates patient positioning.

4.1.2. X-ray Setup

Three components need to be set to simulate an X-ray image. The properties of the X-ray source, the X-ray detector (or cassette) and a virtual anatomy need to be known:

- The *X-ray source* is defined by its position, shape (e.g. parallel beam, point source, or focal spot) and beam spectrum (monochromatic or polychromatic).
- The *X-ray detector* is defined by its position, size, resolution and orientation.
- *Each anatomical structure* is defined by its surface as a triangular mesh and its material properties so

that its linear attenuation coefficients can be computed to solve the Beer-Lambert law. We rely here on Hounsfield values and convert them into mass attenuation coefficients and densities [46].

Other parameters may also be included, e.g. collimation (see below).

In this medical application, whenever possible we favour parameters that are meaningful for the targeted community of users rather than parameters required by the simulator. The user can control the relative distance between the X-ray source and the detector or cassette (known as *source to image distance (SID)* in radiography) and the distance between the X-ray source and the patient (known as *source to object distance (SOD)*). *Centring point* is another technical term used in radiography. Centring is the focus point of the primary X-ray beam in relation to anatomy. This point is dictated by the anatomy that is trying to be demonstrated within an X-ray image. This point will represent the middle of the resultant X-ray.

Centring and positioning of the patient are heavily correlated, and they actually define the relative positions of the X-ray source, of the cassette and of the patient. Therefore appropriate centring and positioning are necessary to maintain the radiation dose to its strict necessary minimum. It is assumed that a radiographer will always ensure that the centre of the body part lies at the middle of the cassette.

Collimation is another common technical term used in radiography. Lead plates or leaves can be placed at the front of the X-ray tube to limit the exposure to ionising radiation to a given area of the body. As lead is a material that heavily attenuates X-rays, hardly any radiation is deposited in the tissues protected by the collimator. Therefore appropriate collimation is also important to ensure the area of interest is definitely included on the image, limit the radiation field to that area of interest, reduce scatter in order to maintain the image quality and limit the radiation exposure of organs at risk (see Figure 6).

Such important aspects of X-ray radiography can be reproduced in our virtual environment. The X-ray source and cassette move as the user moves the mouse in 3D visualisation window. The user can also use the GUI buttons to finely tune the position into a correct centring (see Figure 7). The X-ray beam is represented by the light projection on the patient' skin and cassette (see Figure 6) as it is the case in the X-ray room (see Figure 15(a)).

The X-ray beam spectrum corresponds to a tabulated list of number of photons and corresponding photon en-

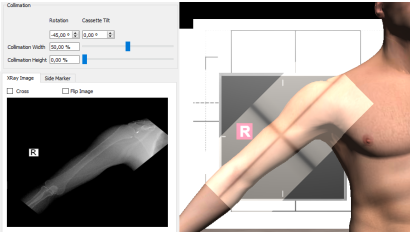


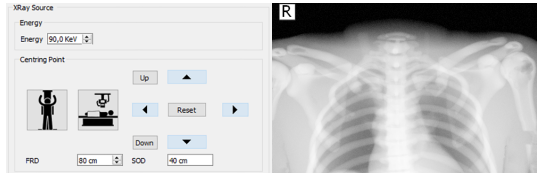
Figure 6: Collimation configuration to target the X-ray beam on the humerus only. It is rotated by 45° and the height of the beam has been reduced.

ergies in kiloelectron volt (keV). In a clinical environment this is controlled by radiographers via the peak kilovoltage (kVp) of the current applied to the X-ray tube. Exposure factors play an important role in X-ray projectional diagnosis because they can affect the quality of the produced radiograph. An inappropriate exposure may decrease the contrast in X-ray images. In order to avoid mistakes and avoid taking the same radiograph several times, trainees must understand how radiation is produced by an X-ray tube and what/how parameters affect the image quality. An X-ray tube contains a cathode to produce electrons and an anode, i.e. a target on which the electrons will collide. If the electrons have a sufficient energy, X-rays will be created. The operator can control the electrical parameters (voltage applied to the tube in kilovolt (kV) and current intensity in milliamperes-second (mAs)) and exposure time in fraction of a second. The voltage controls the energy of the X-ray photons produced by the tube. mAs controls the amount of photons produced over a set amount of time (seconds). For medical diagnosis in radiography, the anode is usually made of tungsten. Voltages in the 55-125 kV range are commonly used in clinical routine. Corresponding spectra can be simulated using the tungsten anode spectral model using interpolating polynomials (TASMIP) algorithm [48]. For each voltage in the range 30-140 kV, it produces a list of photon energies in keV and relative number of photons. The user can select the voltage in kV, and the corresponding beam spectrum is used in the simulation by gVirtualXRay.

Changing the kV value will produce different X-ray images. The X-ray radiation is absorbed differently by soft than dense structures. The level of absorption varies with the photon energy, but not linearly. When the kV increases, the X-ray photons can penetrate more without being absorbed. On the one hand, if the kV value is too low, the image will be whiter and more blurred. On the other hand, if the kV value is too high, the image will be over-exposed and too dark. Our simulator can replicate



(a) X-ray image simulated using a 60 kVp X-ray tube voltage. The incident energy produced by the X-ray tube is too low to sufficiently penetrate the tissues and differentiate them on the X-ray image.



(b) X-ray image simulated using 90 kVp X-ray tube voltage. The contrast between tissues has improved.

Figure 7: Effect of the X-ray tube voltage on an X-ray image of the chest.

such behaviour (see Figure 7).

Note that due to the deterministic nature of the X-ray simulation algorithm, mAs cannot be directly taken into account. However it is possible to mimic a low mAs value by adding Poisson noise to the simulated X-ray image.

4.1.3. Cassette's Side Markers

In clinical radiography, an anatomical marker is placed within the field of the X-ray source, and clear of the area of interest. It aims to identify the left- and right-hand sides of the patient. This is because the left-hand side of the patient may not be on the left of the image. This practice is mandatory to avoid misinterpretation of the X-ray image. In our tool, a 2D widget allows to interactively place a side marker over the cassette using the mouse. This 2D widget transfers this 2D position on the cassette to the 3D visualisation of the cassette in the virtual environment. Additionally, this side marker appears on the X-ray image and can be saved in an image file. See <https://youtu.be/EDJM3pSWtgo> for an illustrative video. Figure 8 shows the side markers in the 3D visualisation and in the corresponding X-ray image.

4.1.4. Digital Image Manipulation

Nowadays, digital X-ray detectors are used in modern hospitals rather than traditional X-ray film. The X-ray image is captured directly to a bitmap by the detector, and it is possible to display it using a computer. The greatest advantage of digital imaging is the ability

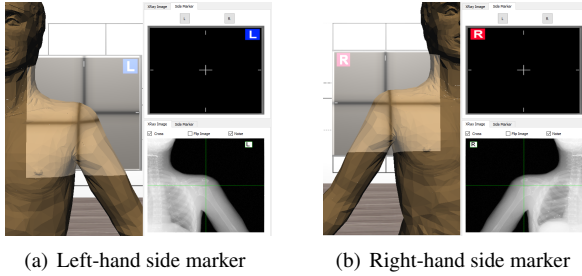
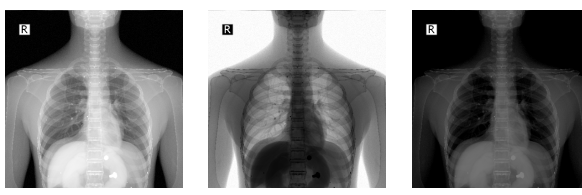


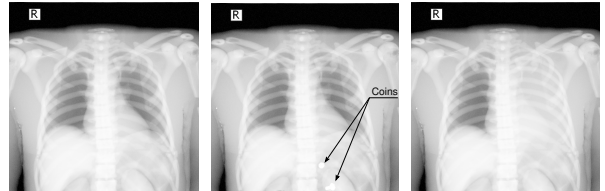
Figure 8: The user can select between the left and right side markers and place it over the cassette.



(a) Normal X-ray image
(b) Same as (a) but using a positive LUT.
(c) Image with a low brightness and a high contrast.

Figure 9: Our tool allows digital image manipulation.

to duplicate, store and manipulate the data. For example, image filtering can be used to reduce minor problems due to overexposure or underexposure, and perform some measurements (e.g. compute the distance between two different anatomical landmarks). Digital images can also be used in computer-aided diagnostic (CAD) software. Our user interface provides a few simple image processing filters that allow users to enhance resulting images (e.g. to get a better interpretation of the anatomical tissues). A Log-Scale filter and a Gamma filter can be selected to improve the final image. The brightness and contrast can also be altered to emphasise each tissue or highlight a particular zone. In medical applications, X-ray images are often shown in *negative*, so that bones are in white and air in black. All these filters can be easily used by clicking with the mouse over the X-ray image. Figure 9 shows examples of image manipulation applied on the same X-ray image. In Figure 9(a), coins can easily be seen on the image compared to Figures 9(b) and 9(c). Also, the anatomical side marker is present to determine the anatomical side of body on the radiographic image. Finally, users can save any X-ray radiograph they want to in an image file on the hard drive. See <https://youtu.be/x7KGsNSMSH8> for a video that focuses on the digital image manipulation.



(a) Normal AP Chest X-ray image.
(b) Same image as (a) but with foreign objects.
(c) Same image as (a) but with a collapsed lung.

Figure 10: The X-Ray attenuation properties of the tissues can be modified to simulate different scenarios.

4.2. Lecturing Features

Our simulator provides additional features which will support the instructor in the classroom environment, although they are not directly related to the simulation of any step of the diagnostic radiography procedure. The system allows to show and hide specific tissues of the virtual patient at run time. For example, the user can modify the opacity of the skin surface to reveal internal structures in the 3D visualisation. This way students can understand the relationship between the different body tissues and X-ray images.

It is also possible to modify the tissues properties with respect to X-ray attenuation using the Hounsfield Scale. Hounsfield values can be converted into list of chemical elements, etc. [46] so that corresponding linear attenuation coefficients can be computed from photon cross-sections [45] to solve the Beer-Lambert law for any incident energy. Being able to change the tissues properties allows teachers to show a variety of diseases, e.g. a calcified bone, a collapsed lung (see Figure 10(c)), or an air-filled stomach. It is even possible to introduce foreign objects inside the internal anatomy. For example, Figures 9 and 10(b) show coins in the stomach. See the following video for further details: <https://youtu.be/02K2ojcExTc>.

4.3. Self-guided Training

Both theoretical and non-cognitive skills are required to perform diagnostic radiographs. The only effective way of acquiring non-cognitive skills is practice. It is now well established that VR resources and computerised simulators can be exploited to guide and boost the trainees' learning process. Interactive tools can also be designed to promote self-directed learning. With this regard, our simulator provides a guided mode that leads users along the procedure. This mode explains the X-ray projection procedure step-by-step and offers additional information if the user requires it. Finally, the

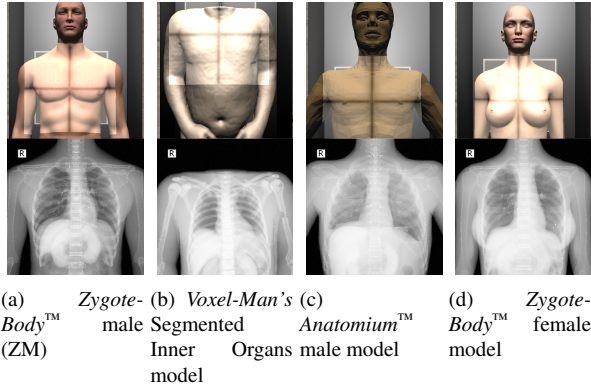


Figure 11: Results obtained using different anatomical models.

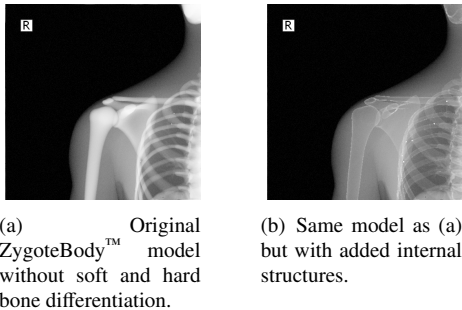


Figure 12: Solving the absence of internal structures in bone.

system evaluates the user’s performance and retrieves assessment metrics. Besides, we offer set of non-guided exercises that allows the instructor to check the evolution of the trainees. Finally, we have created a set of videos to help the users to get used to the simulator. See the following videos for further information: <https://youtu.be/EdyDqvGr8ww> and <https://youtu.be/WFOAVSLxufs>.

5. Results

The proposed X-Ray simulator offers a teaching and learning platform where third party anatomic models can be easily integrated. To test the viability of our approach, we incorporated the following models:

- *ZygoteBody™* 3D Poly Models [12]. This set of virtual patient models provide B-Reps of the most important tissues. We used female (ZF) and male (ZM) models.
- *Anatomium™* 3D Human Anatomy Digital Data Sets [50] offer several virtual patients. Similarly

to *ZygoteBody*, they include the B-reps of several tissues. We used one of the available male models.

- *Voxel-Man’s Segmented Inner Organs* [52, 51]. This model is composed by a set of segmented volumetric images obtained from the Visible Human data set. To incorporate this model, we generate surface meshes using the marching cubes algorithm [53].

Figure 11 depicts the visual results obtained for these models and Table 1 shows the complexity of each model. As it was expected, the quality of the final image depends to a large extend on the quality of the virtual patient model. We found that some general purpose models need further preprocessing to obtain plausible images. Bones are made of two types of tissues. The outer layer of bones is called cortical bones. They are strong and dense. The inner layer, called trabecular bone, is a lot less dense. Commercial 3D virtual models often only provide the bone structures as the surface of the cortical bones. Trabecular bone are almost systematically ignored. Other types of tissues are also provided as their superficial representation, i.e. without nothing inside. However, gVirtualXRay works as a ray tracer where a ray goes through an anatomical structure (front face of a triangle) and get out of the same structure (back face of a triangle) in order to calculate the light attenuation depending on the material properties associated to this anatomical structure and the length of ray crossing it. This solution does not work particularly well with bones because their internal layers attenuate X-rays a lot less. As a consequence, if no particular care is given to bones, they will have an homogeneous look in the simulated X-ray images, which is not very realistic (see Figure 12(a)). To solve this deficiency, we added a new mesh for each bone to depict the trabecular bones. It can be efficiently achieved by duplicating the surface mesh of the cortical bones, shrinking them a little bit, and inverting their normal vectors. Figure 12 depicts the difference between the original meshes without trabecular bones and the modified meshes with trabecular bones. Note that this issue does not occur when working with surface meshes extracted from segmented CT dataset as cortical and trabecular bones are easy to identify and separate in CT data. Regarding the patient positioning, the VPPS module worked seamlessly with all the models used in the evaluation.

VR simulators required interactive frame rates to guarantee an adequate user experience. For this reason, VPPS and gVirtualXRay were implemented to run efficiently in modern GPUs. Besides, both modules share GPU memory to reduce the data transferred through

Table 1: Model complexity.

Model	Superficial Mesh		Volumetric Mesh	
	Vertices	Triangles	Nodes	Tetrahedrons
<i>ZygoteBodyTM</i> Male [49]	1317862	2601469	553412	2576779
<i>ZygoteBodyTM</i> Female [49]	1468989	2896011	492646	2314456
<i>Anatomium</i> Male [50]	790461	1570778	767325	3411170
<i>Segmented Inner Organs</i> [51]	591265	1184325	242033	1182485

the system busses. The performance was tested on an Intel®i7-3770 @ 3.7GHz CPU with 16GB of Random Access Memory (RAM) and a NVIDIA® Quadro K5000 graphics card with 4GB of graphics memory. In the worse case (ZM), the frame rate is over 30 fps. However, the preprocessing module requires about 7 minutes for each virtual patient.

6. Face and Content Validation

A combined face and content validation study has been conducted to gather feedback from experts. The face validation evaluates the level of resemblance between the simulation and the procedure performed in the real world. The content validation quantifies what the tool actually teaches/trains (e.g. psycho-motor skills or anatomy). It ascertains that the simulation correctly replicate the steps and features of the real procedure. Face and content validations are often performed simultaneously using questionnaires. Our questionnaire include questions designed i) to characterise the cohort of participants to assess their level of expertise in X-ray radiography, ii) for the face validation, and iii) for the content validation. The questionnaire is available at <https://goo.gl/forms/HyEIQwedhF8m9XuS2>.

18 participants were recruited. The average number of years of experience is 12.5 years, the standard deviation is 11.74 years: This cohort is well experienced to assess our tool. There are 9 males and 9 females. It allows us to check if there is any gender effect. All the participants but one are qualified. Although most participants were from the United Kingdom (15 of them), 1 participant was from Canada, 1 from France, and 1 from Spain.

16 participants exercise their art in radiography, 1 participant is a medical doctor (MD) in stomatology and another one in nuclear medicine. Due to his specialty, the stomatologist reported be confident when tak-

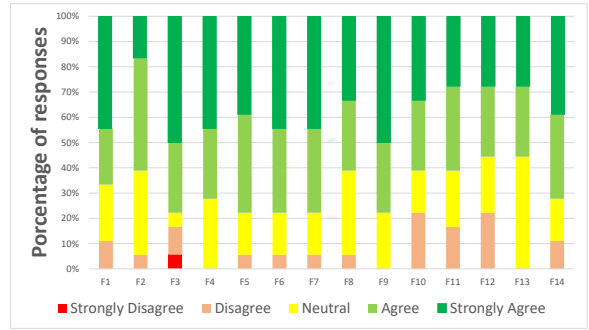


Figure 13: Result of the face validation study using a Likert scale.

ing X-ray radiographs. However, the MD in nuclear medicine did not. Both MDs reported being extremely confident when interpreting X-ray radiographs. As a consequence, their answers were relevant to our study.

14 statements related to the realism of the simulator and its functionalities were used for the face validity (see Table 2). Figure 13 shows the corresponding results for all participants. The percentage of ‘strongly agree’ or ‘agree’ answers for each statement is above 50%. Between 70% and 79% of the participants ‘strongly agree’ or ‘agree’ with seven of the statements (F3, F4, F5, F6, F7, F9, and F14). It is between 60% and 69% for five statements (F1, F2, F8, F10, and F11). It is between 50% and 59% for only two statements (F12 and F13), which are related to the mimicking of disease and the inclusion of foreign objects. This functionality is in its preliminary stage. It was implemented using a relatively naive approach (e.g. changing the HU value for the collapsed lung). The overall feedback is positive (F14). We can conclude that this initial face validation is promising as it clearly shows that most participants ‘strongly agree’ or ‘agree’ that our simulation tool is realistic in many ways.

For content validity, 11 statements related to the main

Table 2: Face validity statements

	Face validity
F1:	The patient model before selecting the posing is visually realistic.
F2:	The deformation of the patient's internal anatomy is visually realistic.
F3:	The previously described steps characterize the procedure in a realistic way.
F4:	The placement of the side markers on the x-ray image is visually realistic.
F5:	The changes in the final x-ray image due to the adjustment of the beam direction and FRD are visually realistic.
F6:	The adjustment of the centre is visually realistic.
F7:	The changes in the final x-ray image due to the collimation adjustment are visually realistic.
F8:	The changes in the final x-ray image due to beam energy configuration are visually realistic.
F9:	In general, the changes in the final x-ray image due to modification of the different parameters are visually realistic.
F10:	The adjustment of the brightness and contrast settings is visually realistic.
F11:	The use of image filters is visually realistic.
F12:	The simulation of diseases is visually realistic.
F13:	The inclusion of foreign objects in the virtual patient is visually realistic.
F14:	Generally speaking, the simulator is visually realistic.

purpose of the simulator and the courseware were included (see Table 3). Figure 14 shows the corresponding results for all participants. A pattern similar to the face validation is observed for the content validation. Between 70% and 79% of the participants ‘strongly agree’ or ‘agree’ with six of the statements (C1, C2, C4, C7, C10, and C11). It is between 60% and 69% for four of the statements (C3, C5, C6, and C8). It is 50% for C9. As our goal is to teach image interpretation, the lower score at F12 and F13 did not affect the content validation. In fact the overall feedback is positive. Participants judged that the tool is useful as a teaching tool for X-ray radiography (C8), but less as a self-guided training tool (C9). However, the results show the suitability of our tool as a teaching tool (C10) and as a self-guided training tool (C11).

Participants also had the opportunity to provide free comments. When provided such comments were very

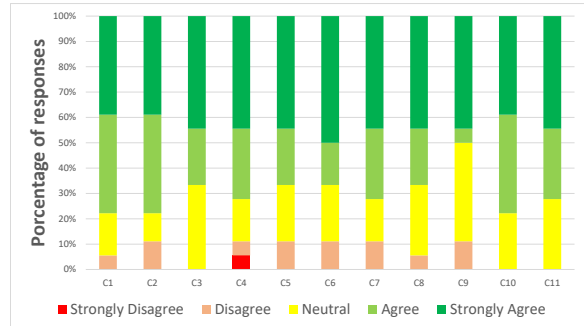


Figure 14: Likert scale responses of content validity.

positive:

“I think this would be a really excellent tool for student to learn from and improve their skills for when they go in placement.”

and

“Great idea”

7. Conclusions

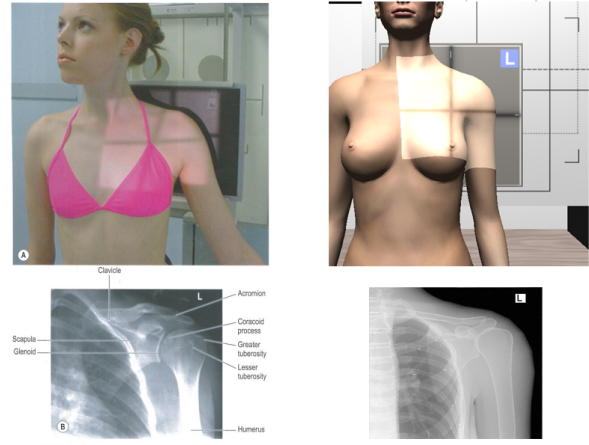
In this paper, we presented a VR teaching and learning environment for diagnostic radiography. It relies on i) an interactive character animation method for the patient positioning and deformation of internal tissues, and ii) a real-time X-ray simulation library. We developed a courseware module that turns our tool into a training system. It is now well established that VR resources and computerised simulators can be exploited to guide and boost the trainees’ learning process. Radiographers have to know both how to position a patient and how to tune an X-ray tube to avoid clinically unnecessary radiation doses and repetitive acquisitions of X-ray images. Our system provides a safe environment where the procedure can be rehearsed, reducing all kinds of radiological risk to the patient or even the radiographer. It is important to highlight that the proposed system does not substitute traditional teaching methods but enhance the learning process overcoming their main limitations. Figure 15 compares a specific projection from a text book [47] with a simulation of the same projection. The real and the virtual patient used to generate both images are also shown. Both, real patient databases and text books are the preferred approaches to get theoretical skills, while our simulator allows to interactively perform the main steps of the procedure in order to train non-cognitive skills.

Table 3: Content validity statements

	Content validity
C1:	Selecting the patient pose from a set of predefined ones is useful for self-guided training.
C2:	Selecting the patient manually is useful for self-guided training.
C3:	Selecting the patient pose from a set of predefined ones is useful to teach the procedure.
C4:	Selecting the patient manually is useful for teaching purposes (e.g. for live demonstration in the lecture theatre).
C5:	Regarding the previously described steps, the simulator is useful to teach the procedure.
C6:	Regarding the previously described steps, the simulator is useful for self-guided training.
C7:	In general, digital image manipulation of the X-ray image is useful for self-guided training and teaching.
C8:	Regarding the functionality described, this is useful to teach the procedure.
C9:	Regarding the functionality described, the simulator is useful for self-guided training.
C10:	Generally speaking, the simulator is suitable is useful as a teaching tool.
C11:	Generally speaking, the simulator is suitable for self-guided training.

We have designed the courseware module to include functionalities to assist the teacher during the lecture and for self-directed learning. Allowing repetitions without any radiation risk, it is useful in both environments. Since, the positioning tool and the X-ray image simulation achieve interactive frame rates, the teachers and students can select the anatomy position and the machine set-up and see the corresponding changes in X-ray image in realtime. In the classroom, teachers can discuss a given procedure, e.g. what is important and the pitfalls to avoid. They can interactively show a good picture (good positioning, centring, collimation, and setting of the X-ray machine) and bad ones. In contrast, the courseware guides the students through the procedure and they can see the actual consequences of their mistakes. Additionally, we provide a non-guided mode, where the system asks the student for an specific projection (see Figure 16)

Our solution was designed to facilitate the incorporation of new virtual patient models. Section 5 shows how several third party models were successfully integrated. This functionality was particularly challenging since our tool allows the user to modify interactively the



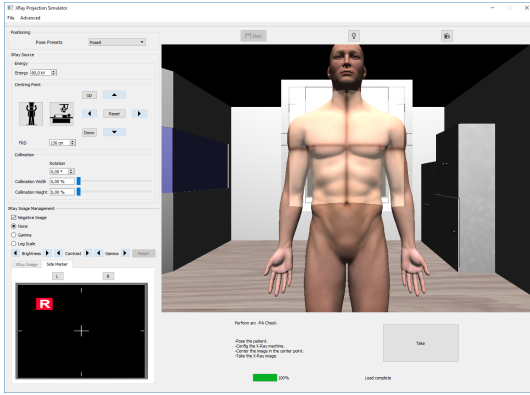
(a) Image courtesy of E. Carver, B. Carver and Elsevier Health Sciences [47].
(b) Projection replicated in the simulator.

Figure 15: Our system can replicate any type of projection, allowing the user to select the patient position and the X-ray configuration.

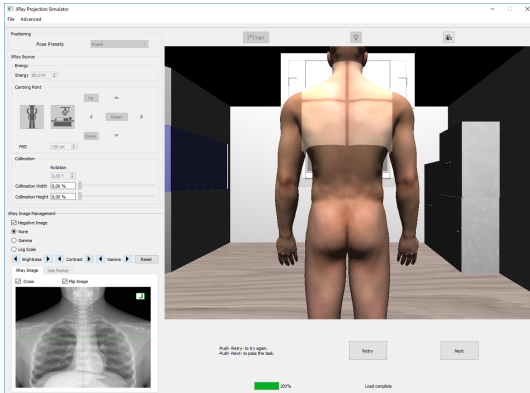
patient's position and very few constraints are imposed to the models. Indeed, only the skin and bone tissues of the virtual patient need to be properly labelled. Currently, the scientific community is putting a lot of effort in developing new techniques for creating virtual patient to be used in VR medical trainers and planners [54, 55]. The proposed X-Ray simulator will benefit from these developments as most of these techniques are compatible with our approach. On the same way, other medical imaging process can be simulated and integrated in the same tool. Recently, there are projects trying to simulate effectively techniques like MRI or CT, which requires some patient position knowledge.

The positioning system sacrifices accuracy in favour of computational performance and flexibility. Natural phenomena such as gravity cannot be simulated. As a result of using a geometrically-based algorithm, its plausible positions are only oriented for training and educational purposes.

We have also conducted a set of experiments to probe the face and content validity of our tool. The overall results of the face validity show that our tool is realistic in many ways. However, the simulation of specific diseases and the inclusion of foreign objects need to be improved. The overall results of the content validity show both the usefulness and suitability of our tool in teaching and/or learning X-ray radiography. However, further tests would be needed to perform a construct validation study, i.e. to assess the actual benefit of using our tool in teaching.



(a) Student must select a position without any hint and take a image without X-ray.



(b) Student can revise the result before next exercises.

Figure 16: GUI in non-guided training mode.

Nevertheless, this tool has some limitations about the full procedure. There are important concerns like the patient preparation which is not covered in this tool:

- Physician must employ appropriate and effective communication with patients
- Patient is indicated about remove clothes or artefacts over the relevant examination area.
- Recommendations about use lead rubber either on patients or radiographers.
- Some assessments which involve medical conditions or protocols like pregnancy, correct patient identification, etc.

Finally, we would like to remark that computerised systems are very good registering the user actions. All this information can be used to develop a set of assessment metric that will serve to provide the trainees with information to boost their self-learning processes and to

evaluate their proficiency. The definition of a valid set of assessment metrics will be explored in our future work.

Acknowledgements

The research leading to these results has been partially funding by the following entities: the Spanish Government [Cajal Blue Brain Project, Spanish partner of the Blue Brain Project initiative from EPFL; and grants TIN2014-57481-C2-1-R, TIN2017-83132-C2-1-R and FPU15/05747] and European Commission [under grant agreements: HBP - Human Brain Project - FET Flagship HBP604102; RaSimAS: Regional Anaesthesia Simulator and Assistant - FP7-ICT 610425, and Fly4PET: Fly Algorithm in PET Reconstruction for Radiotherapy Treatment Planning - FP7-PEOPLE-2012-CIG 321968].

Some examples were based on the Visible Human male data set (National Library of Medicine) and the Segmented Inner Organs (Voxel-Man).

We would like to thanks HPC Wales for the use of its supercomputer during the validation of gVirtualXRay and NVIDIA for donating the GPU that was used during the implementation of gVirtualXRay.

References

- [1] P. Deshpande, A. Rasin, E. Brown, J. Furst, D. Raicu, S. Monter, S. Armato III, An integrated database and smart search tool for medical knowledge extraction from radiology teaching files, in: Proceedings of Workshop on Medical Informatics and Healthcare, 2017, pp. 10–18 (2017).
- [2] R. Spouge, Review of UBC Radiology Teaching App, Journal of Digital Imaging (Oct 2017). doi:10.1007/s10278-017-0034-y.
- [3] A. Bernardo, Virtual reality and simulation in neurosurgical training, World Neurosurgery 106 (2017) 1015–1029 (2017). doi:10.1016/j.wneu.2017.06.140.
- [4] G. S. Ruthenbeck, K. J. Reynolds, Virtual reality for medical training: the state-of-the-art, Journal of Simulation 9 (1) (2015) 16–26 (2015). doi:10.1057/jos.2014.14.
- [5] J. Cecil, A. Gupta, M. Pirela-Cruz, An advanced simulator for orthopedic surgical training, International journal of computer assisted radiology and surgery 13 (2) (2018) 305–319 (2018). doi:10.1007/s11548-017-1688-0.
- [6] P. Korzeniowski, R. J. White, F. Bello, VCSim3: a VR simulator for cardiovascular interventions, International journal of computer assisted radiology and surgery 13 (1) (2018) 135–149 (2018). doi:10.1007/s11548-017-1679-1.
- [7] R. Patel, R. Dennick, Simulation based teaching in interventional radiology training: is it effective?, Clinical Radiology 72 (3) (2017) 266.e7–266.e14 (2017). doi:10.1016/j.crad.2016.10.014.
- [8] P.-F. Villard, F. P. Vidal, L. Ap Cenydd, R. Holbrey, S. Pisharody, S. Johnson, A. Bulpitt, N. W. John, F. Bello, D. Gould, Interventional radiology virtual simulator for liver biopsy, International journal of computer assisted radiology and surgery

- 9 (2) (2014) 255–267 (2014). doi:10.1007/s11548-013-0929-0.
- [9] M. Shanahan, Student perspective on using a virtual radiography simulation, *Radiography* 22 (3) (2016) 217–222 (2016). doi:10.1016/j.radi.2016.02.004.
- [10] P. Bridge, T. Gunn, L. Kastanis, D. Pack, P. Rountree, D. Starkey, G. Mahoney, C. Berry, V. Braithwaite, K. Wilson-Stewart, The development and evaluation of a medical imaging training immersive environment, *Journal of Medical Radiation Sciences* 61 (3) (2014) 159–165 (2014). doi:10.1002/jmrs.60.
- [11] B. Preim, P. Saalfeld, A survey of virtual human anatomy education systems, *Computers & Graphics* 71 (2018) 132–153 (2018). doi:10.1016/j.cag.2018.01.005.
- [12] Zygote Media Group, ZygoteBody, <https://www.zygotebody.com/>, accessed: 2018-11-08 (2018).
- [13] J. E. de Oliveira, P. Giessler, A. Keszei, A. Herrler, T. M. Deserno, Surface mesh to voxel data registration for patient-specific anatomical modeling, in: *Medical Imaging 2016: Image-Guided Procedures, Robotic Interventions, and Modeling*, Vol. 9786, International Society for Optics and Photonics, 2016, p. 978625 (2016). doi:10.1117/12.2217491.
- [14] J. Zhang, J. Chang, X. Yang, J. J. Zhang, Virtual reality surgery simulation: A survey on patient specific solution, in: J. Chang, J. J. Zhang, N. Magnenat Thalmann, S.-M. Hu, R. Tong, W. Wang (Eds.), *Next Generation Computer Animation Techniques*, Vol. 10582 of Lecture Notes in Computer Science, Springer International Publishing, Cham, 2017, pp. 220–233 (2017). doi:10.1007/978-3-319-69487-0_16.
- [15] A. Rajagopal, C. L. Dembia, M. S. DeMers, D. D. Delp, J. L. Hicks, S. L. Delp, Full-body musculoskeletal model for muscle-driven simulation of human gait, *IEEE Transactions on Biomedical Engineering* 63 (10) (2016) 2068–2079 (2016). doi:10.1109/TBME.2016.2586891.
- [16] A.-E. Ichim, P. Kadlecák, L. Kavan, M. Pauly, Phace: Physics-based face modeling and animation, *ACM Trans. Graph.* 36 (4) (2017) 153:1–153:14 (Jul. 2017). doi:10.1145/3072959.3073664.
- [17] Y. Fan, J. Litven, D. K. Pai, Active volumetric musculoskeletal systems, *ACM Trans. Graph.* 33 (4) (2014) 152:1–152:9 (Jul. 2014). doi:10.1145/2601097.2601215.
- [18] T. T. Dao, P. Poulettaut, F. Charleux, Á. Lazáry, P. Eltes, P. P. Varga, M. C. H. B. Tho, Multimodal medical imaging (CT and dynamic MRI) data and computer-graphics multi-physical model for the estimation of patient specific lumbar spine muscle forces, *Data & Knowledge Engineering* 96-97 (2015) 3–18 (2015). doi:10.1016/j.ddata.2015.04.001.
- [19] N. Magnenat-Thalmann, R. Laperrière, D. Thalmann, Joint-dependent local deformations for hand animation and object grasping, in: *Proceedings on Graphics Interface '88*, Canadian Information Processing Society, Toronto, Ont., Canada, Canada, 1988, pp. 26–33 (1988).
URL <http://dl.acm.org/citation.cfm?id=102313.102317>
- [20] L. Kavan, S. Collins, J. Žára, C. O'Sullivan, Skinning with dual quaternions, in: *Proceedings of the 2007 Symposium on Interactive 3D Graphics and Games, I3D '07*, ACM, New York, NY, USA, 2007, pp. 39–46 (2007). doi:10.1145/1230100.1230107.
- [21] N. A. Rumman, M. Fratarcangeli, State of the art in skinning techniques for articulated deformable characters, in: *Proceedings of the 11th Joint Conference on Computer Vision, Imaging and Computer Graphics Theory and Applications: Volume 1: GRAPP*, SCITEPRESS-Science and Technology Publications, Lda, 2016, pp. 200–212 (2016).
- [22] B. H. Le, J. K. Hodgins, Real-time skeletal skinning with optimized centers of rotation, *ACM Trans. Graph.* 35 (4) (2016) 37:1–37:10 (Jul. 2016). doi:10.1145/2897824.2925959.
- [23] A. Sújar, J. J. Casafranca, A. Serrurier, M. García, Real-time animation of human characters' anatomy, *Computers & Graphics* 74 (2018) 268–277 (2018). doi:10.1016/j.cag.2018.05.025.
- [24] I. Baran, J. Popović, Automatic rigging and animation of 3D characters, *ACM Trans. Graph.* 26 (3) (2007) 72:1–72:8 (Jul. 2007). doi:10.1145/1276377.1276467.
- [25] A. Jacobson, I. Baran, J. Popović, O. Sorkine-Hornung, Bounded biharmonic weights for real-time deformation, *Commun. ACM* 57 (4) (2014) 99–106 (Apr. 2014). doi:10.1145/2578850.
- [26] A.-H. Dicko, T. Liu, B. Gilles, L. Kavan, F. Faure, O. Palombi, M.-P. Cani, Anatomy transfer, *ACM Trans. Graph.* 32 (6) (2013) 188:1–188:8 (Nov. 2013). doi:10.1145/2508363.2508415.
- [27] S. Agostinelli, et al., Geant4—a simulation toolkit, *Nucl Instrum Methods Phys Res A* 506 (3) (2003) 250–303 (2003). doi:10.1016/S0168-9002(03)01368-8.
- [28] A. Bielajew, et al., History, overview and recent improvements of EGS4, Tech. rep., Stanford Linear Accelerator Center (SLAC) (2004). doi:10.2172/839781.
- [29] J. Baró, J. Sempau, J. M. Fernández-Varea, F. Salvat, PENELOPE: An algorithm for Monte Carlo simulation of the penetration and energy loss of electrons and positrons in matter, *Nucl Instrum Methods Phys Res B* 100 (1) (1995) 31–46 (1995). doi:10.1016/0168-583X(95)00349-5.
- [30] F. Inanc, J. N. Gray, T. Jensen, J. Xu, Human body radiography simulations: development of a virtual radiography environment, in: *Proc. SPIE*, Vol. 3336, 1998, p. 8 (1998). doi:10.1117/12.317091.
- [31] A. Glière, Sindbad: From CAD model to synthetic radiographs, in: *Review of Progress in Quantitative Nondestructive Evaluation: Volume 17A*, Springer US, Boston, MA, 1998, pp. 387–394 (1998). doi:10.1007/978-1-4615-5339-7_49.
- [32] G.-R. Tillack, C. Bellon, C. Nockemann, Computer simulation of radiographic process - a study of complex component and defect geometry, in: *Review of Progress in Quantitative Nondestructive Evaluation: Volume 14*, Springer US, Boston, MA, 1995, pp. 665–672 (1995). doi:10.1007/978-1-4615-1987-4_82.
- [33] D. Lazos, Z. Kolisti, N. Pallikarakis, A software data generator for radiographic imaging investigations, *IEEE Transactions on Information Technology in Biomedicine* 4 (1) (2000) 76–79 (March 2000). doi:10.1109/4233.826863.
- [34] N. Freud, P. Duvauchelle, J. M. Létang, D. Babot, Fast and robust ray casting algorithms for virtual X-ray imaging, *Nucl Instrum Methods Phys Res B* 248 (1) (2006) 175–180 (2006). doi:10.1016/j.nimb.2006.03.009.
- [35] W. Straßer, Schnelle kurven- und flächendarstellung auf graphischen sichtgeräten, Ph.D. thesis, TU Berlin (1974).
- [36] E. E. Catmull, A subdivision algorithm for computer display of curved surfaces, Ph.D. thesis, The University of Utah (1974).
- [37] F. P. Vidal, M. Garnier, N. Freud, J. M. Létang, N. W. John, Simulation of X-ray Attenuation on the GPU, in: W. Tang, J. Collomosse (Eds.), *Theory and Practice of Computer Graphics*, The Eurographics Association, 2009, pp. 25–32 (2009). doi:10.2312/LocalChapterEvents/TPCG/TPCG09/025-032.
- [38] F. P. Vidal, P.-F. Villard, Development and validation of real-time simulation of x-ray imaging with respiratory motion, *Computerized Medical Imaging and Graphics* 49 (2016) 1–15 (2016). doi:10.1016/j.compmedimag.2015.12.002.
- [39] Q. Gong, R.-I. Stoian, D. S. Coccarelli, J. A. Greenberg, E. Vera, M. E. Gehm, Rapid simulation of x-ray transmission imaging

- for baggage inspection via gpu-based ray-tracing, Nuclear Instruments and Methods in Physics Research Section B: Beam Interactions with Materials and Atoms 415 (2018) 100–109 (2018). doi:10.1016/j.nimb.2017.09.035.
- [40] P. Borosán, M. Jin, D. DeCarlo, Y. Gingold, A. Nealen, RigMesh: Automatic rigging for part-based shape modeling and deformation, ACM Trans. Graph. 31 (6) (2012) 198:1–198:9 (Nov. 2012). doi:10.1145/2366145.2366217.
- [41] C.-H. Huang, E. Boyer, S. Ilic, Robust human body shape and pose tracking, in: Proceedings of the 2013 International Conference on 3D Vision, 3DV '13, IEEE Computer Society, Washington, DC, USA, 2013, pp. 287–294 (2013). doi:10.1109/3DV.2013.45.
- [42] D. M. Beazley, SWIG: An easy to use tool for integrating scripting languages with C and C++, in: Proceedings of the 4th Conference on USENIX Tcl/Tk Workshop, 1996 - Volume 4, TCLTK'96, USENIX Association, Berkeley, CA, USA, 1996, pp. 15–15 (1996). URL <http://dl.acm.org/citation.cfm?id=1267498.1267513>
- [43] J. M. Galvin, C. Sims, G. Dominiak, J. S. Cooper, The use of digitally reconstructed radiographs for three-dimensional treatment planning and ct-simulation, International Journal of Radiation Oncology*Biology*Physics 31 (4) (1995) 935–942 (1995). doi:10.1016/0360-3016(94)00503-6.
- [44] F. P. Vidal, M. Garnier, N. Freud, J. M. Létang, N. W. John, Accelerated deterministic simulation of x-ray attenuation using graphics hardware, in: Eurographics 2010 - Poster, Eurographics Association, Norrköping, Sweden, 2010, p. Poster 5011 (May 2010).
- [45] M. J. Berger, J. H. Hubbell, S. M. Seltzer, J. Chang, J. S. Coursey, R. Sukumar, D. S. Zucker, K. Olsen, XCOM: Photon cross section database, Tech. Rep. NBSIR 87-3597, National Institute of Standards and Technology, Gaithersburg, MD (2010). doi:10.18434/T48G6X. URL <http://physics.nist.gov/xcom>
- [46] W. Schneider, T. Bortfeld, W. Schlegel, Correlation between CT numbers and tissue parameters needed for Monte Carlo simulations of clinical dose distributions, Physics in Medicine & Biology 45 (2) (2000) 459–478 (2000). doi:10.1088/0031-9155/45/2/314.
- [47] E. Carver, B. Carver, Medical Imaging: Techniques, Reflection & Evaluation, 2nd Edition, Elsevier Health Sciences, 2012 (2012).
- [48] J. M. Boone, J. A. Seibert, An accurate method for computer-generating tungsten anode X-ray spectra from 30 to 140 kV, Medical Physics 24 (11) (1997) 1661–1670 (1997). doi:10.1118/1.597953.
- [49] R. Kelc, Zygote body: A new interactive 3-dimensional didactical tool for teaching anatomy, WebmedCentral ANATOMY 3 (1) (2012). doi:10.9754/journal.wmc.2012.002903.
- [50] 21st Century Solutions Ltd, Digital human 3D body anatomy, <http://www.anatomium.com/>, accessed: 2018-11-08.
- [51] Segmented Inner Organs (SIO) Group, Voxel-Man, <https://www.voxel-man.com/segmented-inner-organs-of-the-visible-human/>, accessed: 2018-11-08.
- [52] U. Tiede, A. Pommert, B. Pflessner, E. Richter, M. Riemer, T. Schiemann, R. Schubert, U. Schumacher, K. H. Höhne, A high-resolution model of the inner organs based on the visible human data set, Journal of Visualization 5 (3) (2002) 212–212 (Sep 2002). doi:10.1007/BF03182328.
- [53] W. E. Lorensen, H. E. Cline, Marching cubes: A high resolution 3D surface construction algorithm, SIGGRAPH Comput. Graph. 21 (4) (1987) 163–169 (Aug. 1987). doi:10.1145/37402.37422.
- [54] W. I. M. Willaert, R. Aggarwal, I. Van Herzele, N. J. Cheshire, F. E. Vermassen, Recent advancements in medical simulation: patient-specific virtual reality simulation, World journal of surgery 36 (7) (2012) 1703–1712 (2012). doi:10.1007/s00268-012-1489-0.
- [55] E. Votta, T. B. Le, M. Stevanella, L. Fusini, E. G. Caiani, A. Redaelli, F. Sotiropoulos, Toward patient-specific simulations of cardiac valves: state-of-the-art and future directions, Journal of biomechanics 46 (2) (2013) 217–228 (2013). doi:10.1016/j.jbiomech.2012.10.026.

Appendix A. YouTube Playlist

We provide a YouTube playlist for the reader's convenience. It can be found at https://www.youtube.com/playlist?list=PLI54dBkPi2QjkHx10Z6FCmlDW_kZUAIX. It includes the videos as follows:

- <https://youtu.be/EdyDqvGr8ww> provides an overview of the various steps involved into producing an X-ray image with our tool.
- <https://youtu.be/zitw5-Xk4dY> illustrates the character animation framework and the real-time deformation of internal soft tissues.
- <https://youtu.be/1s-eTT1pCy8> provides evidence of motion capture using the Microsoft Kinect to transfer the position of an actual human being to the virtual patient.
- <https://youtu.be/EDJM3pSWtgo> focuses on the side markers.
- <https://youtu.be/x7KGsNSMSh8> focuses on digital image manipulation of the produced X-ray image.
- <https://youtu.be/02K2ojcExTc> shows special cases (collapsed lung and the insertion of foreign objects).
- <https://youtu.be/GwWY8AQffEY> shows that our tool can be extended to provide students with exercises.
- <https://youtu.be/WFOAVSLXufs> is a longer video, with a summary of the most important functionalities of our tool.